

# Heme Orientation of Cavity Mutant Hemoglobins (His F8? ?Gly) in Either or Subunits: Circular Dichroism, <sup>1</sup>H NMR, and Resonance Raman Studies

著者	Nagai Masako, Nagai Yukifumi, Aki Yayoi, Sakurai Hiroshi, Mizusawa Naoki, Ogura Takashi, Kitagawa Teizo, Yamamoto Yasuhiko, Nagatomo Shigenori
journal or publication title	Chirality
number	1 August 2016
page range	585-592
year	2016-08-01
URL	<a href="http://hdl.handle.net/2297/46156">http://hdl.handle.net/2297/46156</a>

doi: 10.1002/chir.22620

## Heme Orientation of Cavity Mutant Hemoglobins (His F8→Gly) in Either $\alpha$ or $\beta$ Subunits: Circular Dichroism, $^1\text{H}$ NMR, and Resonance Raman Studies

MASAKO NAGAI,<sup>\*1,2</sup> YUKIFUMI NAGAI,<sup>2</sup> YAYOI AKI,<sup>2</sup> HIROSHI SAKURAI,<sup>2</sup> NAOKI MIZUSAWA,<sup>1</sup> TAKASHI OGURA,<sup>3</sup> TEIZO KITAGAWA,<sup>3</sup> YASUHIKO YAMAMOTO,<sup>4</sup> AND SHIGENORI NAGATOMO<sup>\*4</sup>

<sup>1</sup>Research Center for Micro-Nano Technology, Hosei University, Koganei, Tokyo 184-0003, Japan

<sup>2</sup>Department of Health Sciences, Kanazawa University School of Medicine, Kanazawa 920-0942, Japan

<sup>3</sup>Picobiology Institute, Graduate School of Life Science, University of Hyogo, RSC-UH Leading Program Center, Sayogun, Hyogo 679-5148, Japan

<sup>4</sup>Department of Chemistry, University of Tsukuba, Tsukuba, Ibaraki 305-8571, Japan

**ABSTRACT:** Native human adult hemoglobin (Hb A) has mostly normal orientation of heme, whereas recombinant Hb A (rHb A) expressed in *E. coli* contains both normal and reversed orientations of heme. Hb A with the normal heme exhibits positive circular dichroism (CD) bands at both the Soret and 260-nm regions while rHb A with the reversed heme shows a negative Soret and decreased 260-nm CD bands. In order to examine involvement of the proximal histidine (His F8) of either  $\alpha$  or  $\beta$  subunits in determining the heme orientation, we prepared two cavity mutant Hbs, rHb( $\alpha$ H87G) and rHb( $\beta$ H92G) with substitution of glycine for His F8 in the presence of imidazole. CD spectra of both cavity mutant Hbs did not show negative Soret band, but instead exhibited positive bands with strong intensity at the both Soret and 260-nm regions, suggesting that the reversed heme scarcely exists in the cavity mutant Hbs. We have confirmed by  $^1\text{H}$  NMR and resonance Raman (RR) spectroscopies that the cavity mutant Hbs have mainly the normal heme orientation in both the mutated and native one. These results indicate that the heme Fe-His F8 linkage in both  $\alpha$  and  $\beta$  subunits influences the heme orientation, and that the heme orientation of one type of subunits is related to the heme orientation of the complementary subunits to be the same. The present study showed that CD and RR spectroscopies also provided powerful tools for the examination of the heme rotational disorder of Hb A, in addition to usual  $^1\text{H}$  NMR technique.

**KEY WORDS:** heme optical activity, hemoglobin, Soret and 260-nm CD bands, heme rotational disorder, His F8 replaced by Gly, subunit-subunit interaction

**Short Title:** Heme orientation of cavity mutant hemoglobins

**\*Correspondence to:** Masako Nagai, Research Center for Micro-Nano Technology, Hosei University, Koganei, Tokyo 184-0003, Japan, Fax:(+) 81-42-387-5121, E-mail: [masako.nagai.34@hosei.ac.jp](mailto:masako.nagai.34@hosei.ac.jp)  
Shigenori Nagatomo, Department of Chemistry, Graduate School of Pure and Applied Sciences, University of Tsukuba, Tsukuba, Ibaraki 305-8571, Japan, Fax: (+) 81-29-853-6503, E-mail: [nagatomo@chem.tsukuba.ac.jp](mailto:nagatomo@chem.tsukuba.ac.jp)

## INTRODUCTION

We have studied the circular dichroism (CD) spectra of native human adult hemoglobin (Hb A) to elucidate the relationship between its structure and oxygen (O<sub>2</sub>) binding function.<sup>1-10</sup> O<sub>2</sub> binding sites of hemoglobin (Hb) and myoglobin (Mb) are heme (Fe-protoporphyrin IX complex). Heme skeleton is a reflectionally symmetrical molecule and hence optically inactive. However, a prominent positive CD band appears around 400 nm (Soret band) when the heme is incorporated into apoglobin (apoHb or apoMb) *in vivo*. Hb A has mostly normal heme orientation (more than 90%) whereas Hb A reconstituted from apoHb with hemin *in vitro* contained both normal and reversed hemes.<sup>11,12</sup> The heme rotational disorder in reconstituted Hb has been extensively characterized by <sup>1</sup>H NMR spectroscopy.<sup>11-15</sup> Rotation of the heme by 180°, relative to His F8, about the 5,15-meso axis (reversed heme) interexchanges the methyl groups at positions 2 and 7 with the vinyl groups at the positions at 8 and 3, respectively. A <sup>1</sup>H NMR study of Hb A demonstrated the heme orientational ratio of ~ 9:1 favouring the crystallographically characterized form.<sup>12</sup>

However, the reconstituted Hb A prepared from apoHb and hemin *in vitro* contained both the normal and reversed hemes at almost the same population.<sup>11,12</sup> The expression system of recombinant Hb A (rHb A) in *E. coli*, using expression plasmids, pHE2 and pHE7, was described and characterized by Ho's group.<sup>16,17</sup> They reported that some of the heme is not inserted correctly but converted into correct

conformation with an oxidation-reduction process. We used the same expression plasmid, pHE7 which was kindly provided by Professor Ho of Carnegie Mellon University, and demonstrated that rHb A expressed in *E. coli* also contained both the normal and reversed hemes.<sup>18</sup>

Hb A with the normal heme exhibits a positive CD in both Soret and 260-nm regions but rHb A with the reversed heme shows a negative Soret and decreased 260-nm CD bands.<sup>18</sup> The proximal histidine (His F8) directly bound to the heme iron is essential for Hb function. Thus His F8 might be involved in determination of the heme orientation in the pocket. In order to examine the effect of substitution of glycine (Gly) for His F8 on the CD spectrum, we prepared two mutant Hbs, rHb(αH87G) and rHb(βH92G) in the presence of imidazole<sup>19</sup> and their heme orientations were investigated by CD, <sup>1</sup>H NMR and resonance Raman (RR) spectroscopies.

In His F8 mutants of both rMb(H93G) and rHb(αH87G), the location of exogenous imidazole at the proximal pocket has been proven by X-ray crystallography, and the crystallographic data revealed that an imidazole is bound to the heme iron on the proximal site in both mutant Mb and Hb.<sup>20,21</sup>

## MATERIALS AND METHODS

### *Preparation and Purification of Hemoglobins*

Hb A was purified from human hemolysate by preparative isoelectric focusing.<sup>22</sup> The Hb A expression plasmid pHE7,<sup>16</sup> containing human α-

and  $\beta$ -globin genes and the *E. coli* methionine aminopeptidase gene, was used for the synthesis of mutant Hbs.

Cavity mutant Hbs were prepared by site-directed mutagenesis in *E. coli*. The plasmids for rHb( $\alpha$ H87G) and rHb( $\beta$ H92G) were produced using an amplification procedure for closed circular DNA *in vitro*<sup>23</sup> and transformed into *E. coli* JM109. Culture of cells and expression of rHb were the same as reported previously.<sup>19</sup> Recombinant Hbs were purified according to the methods described before.<sup>18,19</sup> We separated the rHb A with reversed heme (in both the  $\alpha$  and  $\beta$  subunits with contents of >80%) from that with normal heme through SP-Sepharose column chromatography.<sup>18</sup> For rHb A containing both the normal and reversed hemes, we used rHb A fractions before the purification by SP-Sepharose column chromatography.

### ***CD Measurements***

The CD measurements were carried out with a Jasco J-820 spectropolarimeter with the same conditions as reported previously.<sup>19</sup> Absorption spectra were measured with a double-beam spectrophotometer (Hitachi, model U-3010). The Hb solution in the ferrous-carbonmonoxy (CO) form, the concentration of which was 45  $\mu$ M (in heme) in 0.05 M phosphate buffer (pH 7.0) containing 5 mM imidazole, was measured at 25 °C with a cell having 2 mm light path-length.

The molar CD ( $\Delta\epsilon$ ) is given in  $M^{-1}cm^{-1}$ , calculated per heme. After conversion into pyridine hemochromogen, molar concentrations

of heme in Hbs were determined spectrophotometrically on the basis of a millimolar extinction coefficient of 34  $mM^{-1}cm^{-1}$  at 557 nm.

### ***<sup>1</sup>H NMR Measurements***

The <sup>1</sup>H NMR spectra were measured with a Bruker AVANCE 400 FT NMR spectrometer operating at the <sup>1</sup>H frequency of 400 MHz. The measurements were performed at 298 K (25 °C). The spectra were recorded using a water suppression method with a presaturation, a 10.2  $\mu$ s 90° pulse, a recycle time of 0.5 s, a spectral width of 36 kHz, 8k data points, and  $\sim$  4k -  $\sim$  8k transients.

The chemical shift of <sup>1</sup>H NMR spectra are given in parts per million relative to sodium 2,2'-dimethyl-2-silapentane-5-sulfonate (DSS), with residual H<sup>2</sup>O as an internal standard. Just before NMR measurements, all of the Hb samples were converted to the met-azido form from CO one and concentrated with a Diaflo membrane.<sup>11,12</sup> The Hb concentrations of Hb A, rHb( $\alpha$ H87G), and rHb( $\beta$ H92G) were 1 mM, 0.3 mM, and 1.7 mM, respectively, on a heme basis. In addition, rHb( $\alpha$ H87G) and rHb( $\beta$ H92G) contained 10 mM imidazole. All Hb samples were measured in 0.02 M phosphate buffer, pH 8.0.

### ***Resonance Raman Measurements***

RR spectra were excited at 441.6 nm with a He/Cd laser (Kinmon Electric, model CD4805R), dispersed with a 1 m single polychromator (Ritsu Oyo Kogaku, model MC-100DG), and detected

with a UV-coated, liquid-nitrogen-cooled CCD detector (Roper Scientific, LN/CCD-1100-PB/VISAR/1). The Hb concentration was 200  $\mu$ M (in heme) in a 0.05 M phosphate buffer (pH 7.0). In addition, rHb( $\alpha$ H87G) and rHb( $\beta$ H92G) contained 10 mM imidazole. The deoxy-form was prepared by adding a small amount of sodium dithionite (1 mg/ml) to the oxy-form after the replacement of the inside air of the sample tube with N<sub>2</sub>. The presented spectra are the sum of 30 exposures, each exposure accumulating data for 10 sec. Raman shifts were calibrated with indene and carbon tetrachloride (CCl<sub>4</sub>) as a frequency standard and the frequency accuracy was  $\pm 1$  cm<sup>-1</sup> for well-defined Raman bands. The integrity of the sample was carefully confirmed by the visible absorption spectra measured before and after the RR measurements. Visible absorption spectra were recorded with a Hitachi U-3310 spectrophotometer. All measurements were carried out at room temperature with a spinning cell (1800 rpm). The laser power at the scattering point was 4.0 mW.

## RESULTS AND DISCUSSION

### Absorption Spectra and Oxygen Binding Properties of Cavity Mutant Hbs

Absorption spectra of rHb( $\alpha$ H87G) and rHb( $\beta$ H92G) were similar to those of Hb A in all the oxy, deoxy, and CO forms (Supporting Information, Fig. S1). Only the slight blue-shift of absorption peaks were observed in the spectra of rHb( $\beta$ H92G) (Table S1).

As shown in the previous paper,<sup>19</sup> rHb( $\alpha$ H87G) displayed a biphasic O<sub>2</sub> binding curve consisting of a high O<sub>2</sub> affinity component (mutated  $\alpha$  subunits) and a low O<sub>2</sub> affinity one (native  $\beta$  subunits). No cooperativity, no Bohr effect and no apparent effect by an allosteric effector (inositol hexaphosphate, IHP) were observed. In contrast, rHb( $\beta$ H92G) showed a simple Hill plot with a high O<sub>2</sub> affinity and no cooperativity, no alkaline Bohr effect and a small effect by IHP.<sup>19</sup> These results suggested that His F8 residues of both  $\alpha$  and  $\beta$  subunits are essential for cooperative O<sub>2</sub> binding of Hb A in a manner that the heme Fe-His F8 bond of  $\alpha$  subunit contributes to increase the O<sub>2</sub> affinity of  $\beta$  subunit through the quaternary structure change, and that of  $\beta$  subunit, on the other hand, decreases the O<sub>2</sub> affinity of  $\alpha$  subunit.<sup>19</sup>

### CD Spectra of Cavity Mutant Hbs

We were able to separate rHb A with the reversed heme from that with the normal one by a SP-Sepharose column chromatography.<sup>18</sup> Inset of Fig. 1A shows CD spectra of CO form of Hb A with the normal and reversed heme.<sup>18</sup> Although Hb A with the normal heme shows distinct positive CD bands at both the Soret and 260-nm regions, rHb A with the reversed heme exhibits a negative CD band at the Soret region and a very small CD band at  $\sim 260$  nm.

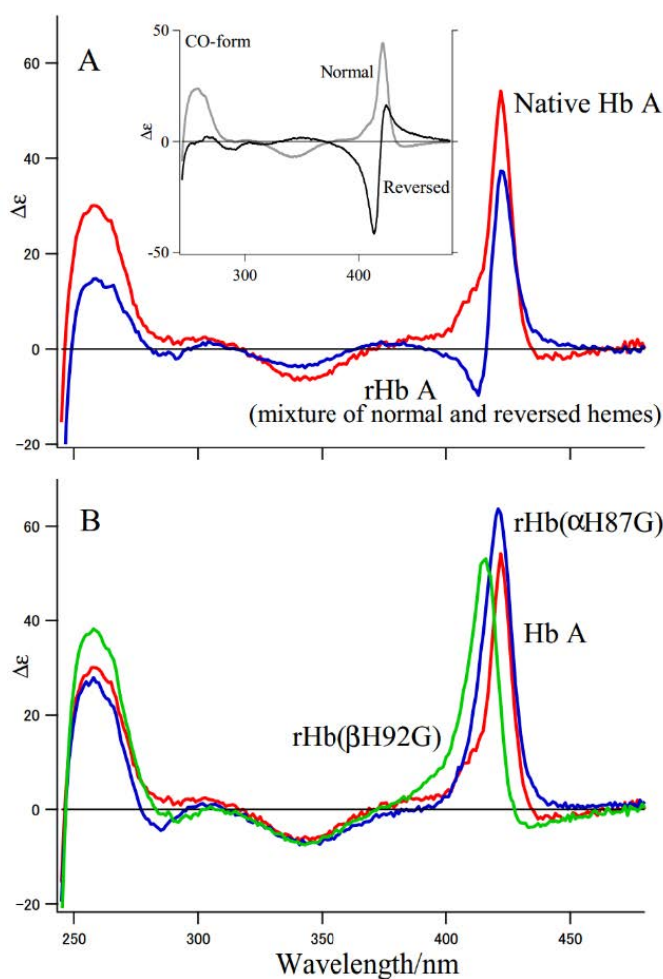


**Fig. 1.** CD spectra of Hb A, rHb A (mixture of normal and reversed hemes) (A), and cavity mutant Hbs (B) in CO forms. CD spectra of Hb (45  $\mu$ M in heme) in 0.05 M phosphate buffer (pH 7.0) were measured in a cell with a light path length of 2 mm. The scan speed was 50 nm/min and 20 scans were averaged. The solution of cavity mutant Hbs were containing 5 mM imidazole. Inset figure in (A) was referred from the previous paper.<sup>18</sup> (A) Red, native Hb A; blue, rHb A before purification by SP-Sepharose column chromatography (mixture of normal and reversed heme orientations).<sup>18</sup> (B) Red, Hb A; blue, rHb( $\alpha$ H87G); and green, rHb( $\beta$ H92G).

Fig. 1A compares the CD spectra of native Hb A with that of rHb A which is a mixture of the normal and reversed hemes before SP-Sepharose column chromatography. Hb A shows a prominent positive CD bands for both the Soret and 260-nm regions, while rHb A exhibits a complex CD with a positive and a negative peaks

in the Soret region and a decreased positive CD band at 260 nm.

Fig. 1B compares CD spectra of rHb( $\alpha$ H87G) and rHb( $\beta$ H92G) with that of Hb A. Both the cavity mutant Hbs show a prominent positive CD band in the Soret region but almost no negative band was able to be observed. In addition, the positive CD bands at  $\sim$  260 nm of both the cavity mutants are alike and similar to that of Hb A.

These results suggest that in the cavity mutant Hbs the reversed heme does not exist not only in the mutated subunits but also in the native ones.

### $^1\text{H}$ NMR Spectra of Cavity Mutant Hbs

The heme rotational disorder in reconstituted Hb A prepared from apoHb and hemin *in vitro* has been extensively characterized by  $^1\text{H}$  NMR spectroscopy.<sup>11-15</sup> The presence of an analogous heme disorder was also demonstrated in the rHb A produced by *E. coli*.<sup>18</sup> To confirm whether reversed heme exists or not in the cavity mutant Hbs, we measured paramagnetically-shifted  $^1\text{H}$

NMR signals of met-azido forms of rHb( $\alpha\text{H87G}$ ) and rHb( $\beta\text{H92G}$ ). Fig. 2 shows the downfield-shifted portions of the 400 MHz  $^1\text{H}$  NMR spectra in the met-azido form of native Hb A (A), rHb( $\alpha\text{H87G}$ ) (B), and rHb( $\beta\text{H92G}$ ) (C). In Hb A (Fig. 2A), two sets of heme methyl proton signals were resolved below 13 ppm, each set arising from the  $\alpha$  or  $\beta$  subunits. Peaks A, C, E and B, D, F were assigned to heme methyl protons of  $\alpha$  and  $\beta$  subunits, respectively.<sup>11,24,25</sup> Thus,  $^1\text{H}$  NMR spectra of paramagnetic met-azido Hb A enable us to discriminate and analyze each subunit.

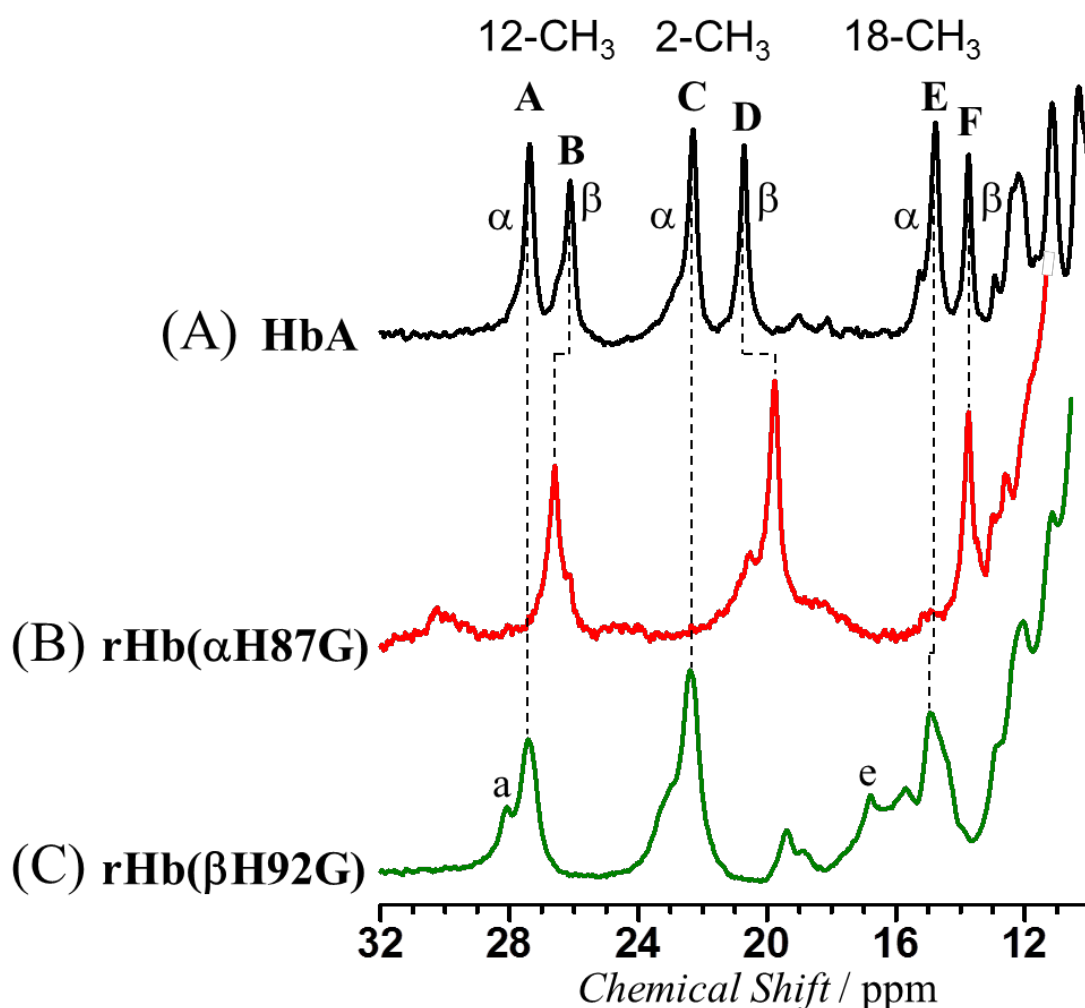


**Fig. 2.** Downfield-shifted region of the 400 MHz  $^1\text{H}$  NMR spectra of the met-azido forms of Hb A (A), rHb( $\alpha\text{H87G}$ ) (B), and rHb( $\beta\text{H92G}$ ) (C) in a 90%  $\text{H}_2\text{O}/10\%$   $^2\text{H}_2\text{O}$  mixture and 0.02 M phosphate buffer, pH 8.0 at 25 °C. Resolved signals A-F have been assigned as follows: heme 12- $\text{CH}_3$  (A), 2- $\text{CH}_3$  (C), and 18- $\text{CH}_3$  (E) for the normal heme of the  $\alpha$  subunit, heme 12- $\text{CH}_3$  (B), 2- $\text{CH}_3$  (D), and 18- $\text{CH}_3$  (F) for the normal heme of the  $\beta$  subunit, and heme 18- $\text{CH}_3$  (a), and 12- $\text{CH}_3$  (e) for the reversed heme of the  $\alpha$  subunit.<sup>11,24,25,42,43</sup>

The individual heme methyl proton signals of Fig. 2A were further assigned to 12- $\text{CH}_3$  (A and B), 2- $\text{CH}_3$  (C and D), and 18- $\text{CH}_3$  (E and F) in each subunit.<sup>11,24,25</sup>

$^1\text{H}$  NMR studies of paramagnetic Hbs have revealed that the metastable intermediate with heme rotated  $180^\circ$  about the 5,15-meso axis (the reversed heme) is formed when Hb is prepared through the reconstitution of apoHb or aporHb expressed in *E. coli*<sup>18</sup> with hemin. In the  $^1\text{H}$  NMR spectrum of rHb A possessing both the normal and reversed hemes, in addition to peaks A-F, six additional peaks, due to 18- $\text{CH}_3(\alpha)$ , 18- $\text{CH}_3(\beta)$ , 8-vinyl  $\text{C}_\alpha\text{H}(\alpha)$ , 8-vinyl  $\text{C}_\alpha\text{H}(\beta)$ , 12- $\text{CH}_3(\alpha)$ , and 12- $\text{CH}_3(\beta)$  of the reversed heme ( $\alpha$  and  $\beta$  in the parentheses indicate the subunit) were observed below 13 ppm.<sup>12,18</sup>

In the  $^1\text{H}$  NMR spectrum of rHb( $\alpha\text{H87G}$ ) (Fig. 2B), signals only from  $\beta$  subunits were observed and their chemical shifts were similar to those of heme 12-, 2-, and 18- $\text{CH}_3$  signals of Hb A, although 12- $\text{CH}_3$  and 2- $\text{CH}_3$  signals of rHb( $\alpha\text{H87G}$ ) were down- and up-field shifted by  $\sim 0.5$  and  $\sim 1$  ppm relative to the corresponding

ones of Hb A. Therefore it was suggested that the heme electronic structure of the  $\beta$  subunit of rHb( $\alpha\text{H87G}$ ) is almost the same as that of the  $\beta$  subunit of Hb A. Furthermore, the absence of the signals due to the reversed heme in the native  $\beta$  subunits of rHb( $\alpha\text{H87G}$ ) indicated that these subunits have only the normal heme.

$^1\text{H}$  NMR spectrum of rHb( $\beta\text{H92G}$ ) (Fig. 2C) exhibited 12- $\text{CH}_3(\alpha)$ , 2- $\text{CH}_3(\alpha)$ , and 18- $\text{CH}_3(\alpha)$  signals with their shifts almost identical to those of the corresponding ones in the spectrum of Hb A, suggesting that the heme electronic structures of the  $\alpha$  subunits of rHb( $\beta\text{H92G}$ ) and Hb A are highly alike. However, the native  $\alpha$  subunits of rHb( $\beta\text{H92G}$ ) exhibited several additional signals (major ones are labeled as a and e) due to the reversed heme (Fig. 2C). Analysis of the intensities of peaks a and A indicated that the native  $\alpha$  subunit of rHb( $\beta\text{H92G}$ ) contains the two heme orientations with a ratio of 4:1 (normal heme:reversed heme).

NMR signals due to heme methyl protons from the mutated  $\alpha$  subunit in rHb( $\alpha\text{H87G}$ ) were not observed in the indicated shift region. Heme methyl signals for the mutated subunits appeared



to shift away from this shift region. In the NMR spectrum of rHb( $\beta$ H92G) (Fig. 2C), peaks were observed at 19.4, 18.9 and 15.7 ppm, together with overlapped signals around 23 and 14 ppm, and they are possibly due to heme methyl protons from the mutated  $\beta$  subunit.

### Resonance Raman Spectra

#### *Spectral comparison between resonance Raman spectra of the normal and reversed hemes in rHb*

##### A

Recently we proposed that orientation of the peripheral groups of heme, especially the 13,17-propionate groups of protoheme, gave a great influence on the Soret CD band.<sup>26</sup> As shown in the previous paper, we were able to decompose the spectrum of rHb A into three types of fractions separated by a SP-Sepharose column chromatography using an intensity of positive CD band at  $\sim 260$  nm<sup>18</sup>; SP-1, SP-2, and SP-3. These fractions showed different CD spectra from each other; SP-1 (the normal heme), a prominent positive Soret CD similar to Hb A, SP-2 (a mixture of the normal and reversed hemes), a complex Soret CD with a positive and a negative band, SP-3 (mainly the reversed heme), a prominent negative Soret CD (see Fig. 1, inset).

The reversed heme brings about a structural interexchange of the 2,7-methyl groups with 3,8-vinyl groups, but no changes about 13,17-propionate groups, because 13,17-propionates are equivalent to 17,13-propionates. However, it is possible to change the direction of 13,17-propionate groups between the normal and reversed hemes. In X-ray structure of Hb A (oxy or CO form), the orientations of heme propionate side chains alternate, i.e., above and below the heme plane (antiparallel conformation) and extend toward one side of heme plane (parallel conformation) in the  $\alpha$  and  $\beta$  subunits, respectively.<sup>27</sup> The Soret CD is possibly affected by the conformations of the 13,17-propionates side chains such as the antiparallel and parallel ones. To get theoretical basis for the contribution of 13,17-propionate side chains conformations to the Soret CD band, we investigated the CD spectra by performing theoretical calculation with a time dependent density functional theory level. The results indicated that the antiparallel conformation of the 13,17-propionate side chains is expected to yield positive rotational strengths but the parallel conformation does negative ones.<sup>26</sup>

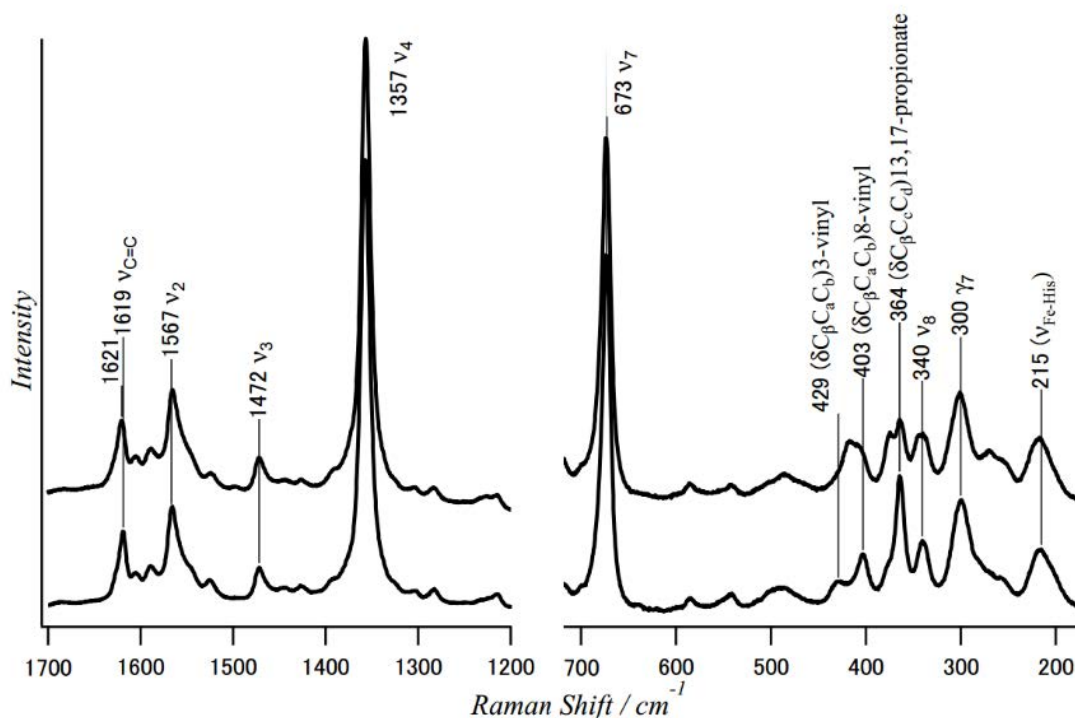


**Fig. 3.** The 441.6-nm excited RR spectra of native Hb A (lower spectrum), rHb A with the reversed heme (upper spectrum) in the deoxy form. The Hb concentration was 200  $\mu\text{M}$  (in heme) in 0.05 M phosphate buffer, pH 7.0. Left panel, RR spectra in the high frequency region; right panel, RR spectra in the low frequency region. Intensities of RR spectra in the low frequency region are three-fold scaled up relative to those of the RR spectra in the high frequency region.

To characterize conformational changes of the 13,17-propionate side chains in the normal and reversed hemes, we compared the 441.6-nm excited RR spectrum of Hb A having the normal heme with that of rHb A having the reversed one (SP-3) in the deoxy form in Fig. 3. All RR bands are derived from the vibrational modes of the deoxy-heme. Assignments were referred to the previous studies.<sup>28-30</sup> The strong  $\nu_4$  band at 1357  $\text{cm}^{-1}$  is known as an oxidation state marker and varies depending on the oxidation state of heme iron. Besides the oxidation state marker ( $\nu_4$ ) in the high frequency region (Fig. 3, left), marker

bands for spin- ( $\nu_2$ ,  $\nu_3$ ), and coordination-states ( $\nu_2$ ,  $\nu_3$ ) of heme iron appear.<sup>28</sup> In the higher frequency region, RR bands of rHb A with the reversed heme were similar to those of Hb A with the normal heme (Fig. 3, left). In the low frequency region, the methine wagging mode ( $\gamma_7$ ) around 300  $\text{cm}^{-1}$ , and the pyrrole stretching ( $\nu_8$ ) at 340  $\text{cm}^{-1}$  were similar between Hb A and rHb A with the reversed heme (Fig. 3, right). However, the RR bands involving the bending character of the propionate methylene groups  $\delta(\text{C}_\beta\text{-C}_\gamma\text{-C}_\delta)$  at 364  $\text{cm}^{-1}$  and the  $\text{C}_\beta\text{-C}_\alpha\text{-C}_\beta$  bending character of the vinyl groups  $\delta(\text{C}_\beta\text{-C}_\alpha\text{-C}_\beta)_{3\text{-vinyl}}$  at 429  $\text{cm}^{-1}$  and

$\delta(C_{\beta}-C_a-C_b)_{8\text{-vinyl}}$  at  $403\text{ cm}^{-1}$ , which are observed for Hb A with the normal heme, are distinctly different from those observed for rHb A with the reversed heme (Fig. 3, upper spectrum). Here, subscripts a, b and c, d describe carbon atoms of vinyl groups, ( $-C_aH=C_bH_2$ ) and of propionate groups ( $-C_cH_2C_dH_2COOH$ ), respectively.

Characteristic RR bands of 3, 8-vinyl groups  $\delta(C_{\beta}-C_a-C_b)$  of Hb A appear at  $403$  and  $429\text{ cm}^{-1}$ , but merge into one band around  $418\text{ cm}^{-1}$  in the spectrum of rHb A with the reversed heme. Furthermore, a single band of the 13,17-propionate groups  $\delta(C_{\beta}-C_c-C_d)_{13,17\text{-propionate}}$  of Hb A at  $364\text{ cm}^{-1}$  splits into two bands at  $364$  and  $374\text{ cm}^{-1}$  in the spectrum of rHb A with the reversed heme as shown in Fig. 3, upper spectrum. These RR differences between the normal and reversed hemes imply a distortion of the heme peripheral groups of the rHb A with the reversed heme, especially in both the vinyl and propionate groups, but no change on the  $\nu_{Fe-His}$  band.

These distinct characters shown by the RR spectra of deoxyHb A have also been observed for

### **Resonance Raman spectra of cavity mutant Hbs**

Fig. 4 shows the  $441.6\text{ nm}$ -excited RR spectra of Hb A (A), rHb( $\alpha$ H87G) (B), and rHb( $\beta$ H92G) (C) in the deoxy-form. In the high frequency region (Fig. 4, left), all RR spectra of Hb A (A, black), rHb( $\alpha$ H87G) (B, red) and rHb( $\beta$ H92G) (C, green) are similar. However, there are some minor differences among them as mentioned below. Bands observed at  $1228\text{ cm}^{-1}$  in the spectra

of the CO-form (Fig. S2, Supporting Information). In Fig. S2, the Fe-CO stretching band ( $\nu_{Fe-CO}$ ) at  $505\text{ cm}^{-1}$  and Fe-C-O bending mode,  $\delta(Fe-C-O)$ , at  $581\text{ cm}^{-1}$  were the same between Hb A with the normal heme and rHb A with the reversed heme, but the vinyl C=C stretching modes ( $\nu_{C=C}$ ) observed at  $\sim 1620$  and  $\sim 1630\text{ cm}^{-1}$  were different between them.

Kincaid's group<sup>31,32</sup> also showed similar observations of RR spectrum for Mb with the normal heme and reconstituted Mb with the reversed one. They obtained RR spectra of Mb with the reversed heme examining by the difference spectra between native Mb and 30 min after reconstitution of Mb from apoMb and hemin<sup>31</sup> and showed distinct frequency shifts and intensity changes of propionate and vinyl bending modes but no changes for  $\nu_{Fe-His}$  mode of Mb with the reversed heme.<sup>32</sup> On the basis of their results, we were able to distinguish the RR spectrum of a sample in question between the normal and reversed hemes from our RR spectra in the low frequency region.

of rHb( $\alpha$ H87G) and rHb( $\beta$ H92G) have slightly larger intensities comparing with that of Hb A, possibly reflecting a difference in the heme propionate side chain conformations between the two mutant Hbs and Hb A. Intensities of band at  $1607\text{ cm}^{-1}$  and  $1500\text{ cm}^{-1}$  in the spectrum of rHb( $\alpha$ H87G) were also larger than those of Hb A. An oxidation state marker band,  $\nu_4$ , of rHb( $\alpha$ H87G) was lower by  $2\text{ cm}^{-1}$  relative to that

of Hb A. The result may also reflect small differences of conformation of heme peripheral

side chains.

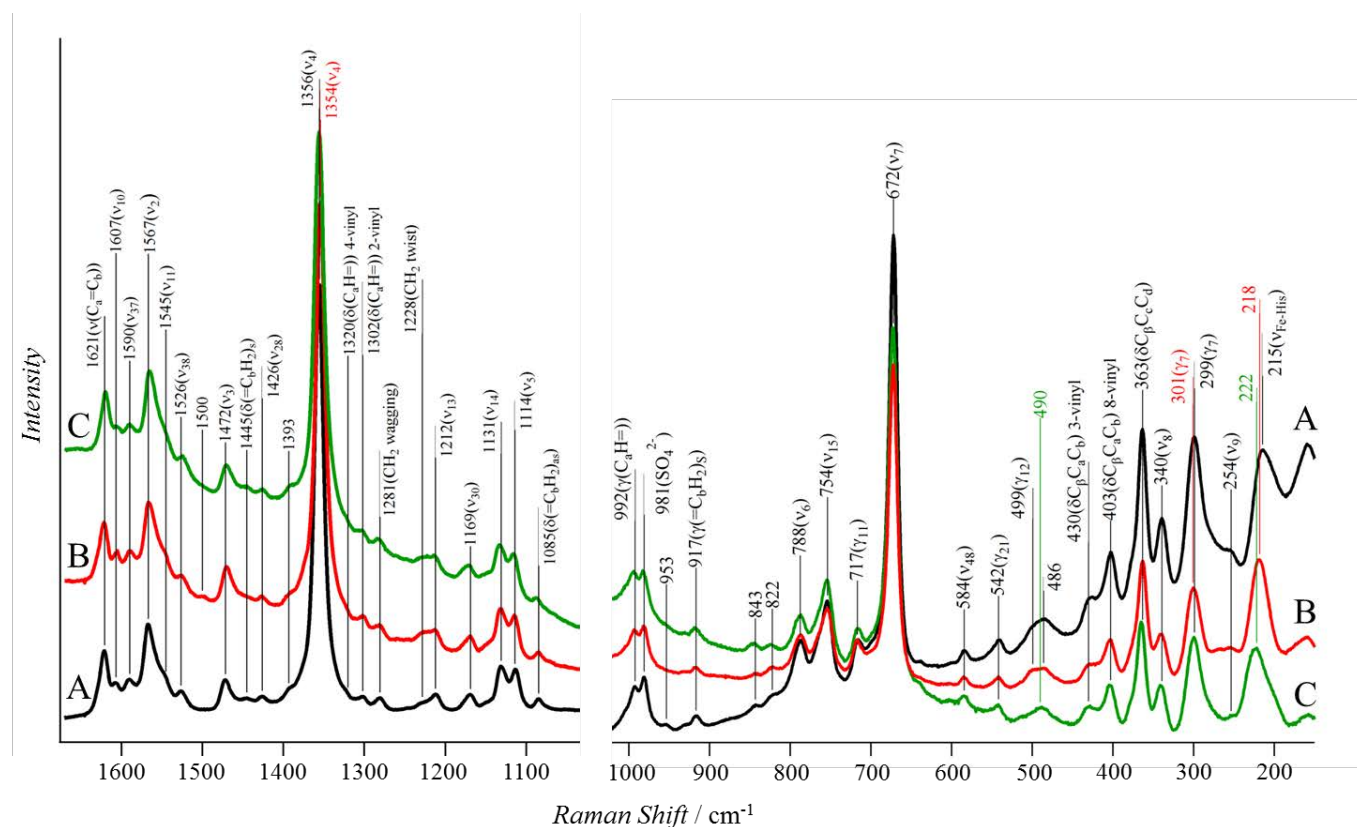


**Fig. 4.** The 441.6-nm excited RR spectra of Hb A (A: black spectrum), rHb(αH87G) (B: red spectrum), and rHb(βH92G) (C: green spectrum) in the deoxy form. The Hb concentration was 200 μM (in heme) in 0.05 M phosphate buffer, pH 7.0. Both rHb(αH87G) and rHb(βH92G) contained 10 mM imidazole. Left panel, RR spectra in the high frequency region; right panel, RR spectra in the low frequency region. Intensities of RR spectra in the low frequency region are 3-fold scaled up relative to those of the RR spectra in the high frequency region.

In the low frequency region (Fig. 4, right), except for the bands around 220 cm<sup>-1</sup> assignable to the Fe-His (ν<sub>Fe-His</sub>) stretching, frequencies of all the other bands were almost similar among Hb A and two mutant Hbs. As shown in Fig. 4, the RR bands involving the C<sub>β</sub>-C<sub>c</sub>-C<sub>d</sub> bending character of the propionate methylene groups δ(C<sub>β</sub>-C<sub>c</sub>-C<sub>d</sub>) at

363 cm<sup>-1</sup> and the C<sub>β</sub>-C<sub>a</sub>-C<sub>b</sub> bending character of the vinyl groups δ(C<sub>β</sub>-C<sub>a</sub>-C<sub>b</sub>)<sub>3-vinyl</sub> at 430 cm<sup>-1</sup> and δ(C<sub>β</sub>-C<sub>a</sub>-C<sub>b</sub>)<sub>8-vinyl</sub> at 403 cm<sup>-1</sup> of both rHb(αH87G) and rHb(βH92G) are almost the same as those of native Hb A, indicating that the reversed heme scarcely exists in the two cavity mutant Hbs in either the mutated subunits or native ones. In

rHb( $\beta$ H92G), although reversed form of 20% in the native  $\alpha$  subunits was contained as shown in Fig. 2, normal and reversed forms in all subunits are 18:2 (9:1), considering that an orientation of

The band assignable to the  $\nu_{\text{Fe-His}}$  ( $215 \text{ cm}^{-1}$  in deoxyHb A) was observed at  $218$  and  $222 \text{ cm}^{-1}$  in the spectra of deoxy-rHb( $\alpha$ H87G) and deoxy-rHb( $\beta$ H92G), respectively. The  $\nu_{\text{Fe-His}}$  band has been usually observed around  $214$ - $218 \text{ cm}^{-1}$  and  $220$ - $224 \text{ cm}^{-1}$  for the typical T (tense) and R (relaxed) states of deoxyHbs, respectively,<sup>33-35</sup> and therefore has been used often for diagnosis of whether quaternary structure of a sample Hb in question is in the T or R state. According to this criteria, rHb( $\alpha$ H87G) and rHb( $\beta$ H92G) in the deoxy-form are in T and R states, respectively, being consistent with their  $\text{O}_2$  binding properties.<sup>19</sup> The mutant Hbs contain subunits that have heme bound to the protein via Fe-His bond, and also subunits that contain heme bound to imidazole via Fe-Im linkage. It is possible that the imidazole-bound deoxy heme might give rise to the  $\nu_{\text{Fe-Im}}$  mode in the same region as the  $\nu_{\text{Fe-His}}$  ones. In the previous papers about heme model compounds, which contain picket fence porphyrin coordinating 1-methylimidazole and 2-methylimidazole,  $\nu_{\text{Fe-Im}}$  was observed between  $222$  and  $225 \text{ cm}^{-1}$ .<sup>36,37</sup> Therefore, we assumed the presence of  $\nu_{\text{Fe-Im}}$  band having a Gaussian shape at  $223 \text{ cm}^{-1}$ , as observed in the mutated subunits of rHb( $\alpha$ H87G) and rHb( $\beta$ H92G). We subtracted the simulated  $\nu_{\text{Fe-Im}}$  band from the observed  $\nu_{\text{Fe-Im}}$  band, and we regarded the remaining bands as Fe-His bands of

the mutated  $\beta$  subunits in rHb( $\beta$ H92G) is almost normal from CD result as shown at Fig.1.

Therefore, we consider that characteristic bands for reversed form did not appear.

the native subunits of rHb( $\alpha$ H87G) and rHb( $\beta$ H92G), respectively, which correspond  $\nu_{\text{Fe-His}}$  of the native  $\beta$  and  $\alpha$  subunits, respectively. The subtracted remaining bands of rHb( $\alpha$ H87G) and rHb( $\beta$ H92G) in deoxy form showed peaks at  $217 \text{ cm}^{-1}$  ( $\nu_{\text{Fe-His}}$  in  $\beta$  subunit) and  $222 \text{ cm}^{-1}$  ( $\nu_{\text{Fe-His}}$  in  $\alpha$  subunit), respectively.<sup>19</sup>

There are some small differences in  $\gamma_7$  ( $\sim 300 \text{ cm}^{-1}$ ),  $\gamma_{12}$  ( $\sim 500 \text{ cm}^{-1}$ ) and  $\nu_4$  ( $\sim 1355 \text{ cm}^{-1}$ ) bands among Hb A, Hb( $\alpha$ H87G) and rHb( $\beta$ H92G). According to Podstawka *et al.*,<sup>38</sup> the frequency of the  $\gamma_7$  band depends on distortion of methine carbons. The  $\gamma_{12}$  band is assigned to the pyrrole swiveling modes.<sup>28</sup> It is indicated that the out-of-plane modes,  $\gamma_7$  and  $\gamma_{12}$ , become Raman active in the high-spin complexes,<sup>28</sup> although they should be inactive for the planar- $D_{4h}$  structure. The  $\nu_4$  reflects an oxidation state of heme iron as previously mentioned.<sup>28</sup> These results may suggest that environments of heme pockets are different among Hb A and the two mutant Hbs, but practically the differences are relatively small among the three Hbs.

We used three different methods to examine the heme rotational disorder of rHbs, i.e., NMR, RR, and CD. Each measurement needs appropriate sample conditions: sample concentration, pH, and ligation state of the protein; for  $^1\text{H}$  NMR, concentrated sample (mM of heme), at pH 8 in the

case of met-azido form; for RR, sample concentration of 200  $\mu\text{M}$  in heme with deoxy form at pH 7; for CD, concentration of 45  $\mu\text{M}$ , ferrous-CO form at pH 7. Usually, 10 mM imidazole was added to the sample solution, but 5 mM was used for CD measurement, because imidazole has an absorption in UV region, but CD in the Soret region was not different between 5 and 10 mM imidazole. The stability of rotational isomers of reconstituted Hb is highly dependent on oxidation and ligation states of heme. Aquo-met form is most unstable and easily changed from the reversed heme to the normal ones (half-life time, <10 h). In contrast, met-azido form or ferrous-CO forms are stable for long time (half-life time, <150 d).<sup>12</sup> The reversed heme is stable in met-azido, ferrous-CO and deoxy forms at neutral pH (pH 7 - 8)<sup>12</sup>, and therefore, there might be no change in the ratio between the normal and the reversed hemes during the measurements performed under the experimental conditions used in the present study.<sup>12</sup>

### Possible Mechanism of Heme Insertion into Apohemoglobin

X-ray studies have provided precise information on details of the heme-globin linkage.<sup>39</sup> The heme is inserted in a cleft between the E and F helices. The heme iron is linked through a coordination bond with imidazole nitrogen of the proximal His F8. The heme is oriented in such a way that one side of the heme plane with the asymmetrically attached nonpolar vinyl groups is buried deep in the hydrophobic

interiors of the cleft, while on the other side of the heme plane the charged propionate side chains are oriented toward hydrophilic surface of the protein moiety. In addition, the heme is stabilized in the inside of the cleft by a large number of van der Waals contacts with side chains of nearby residues.<sup>39</sup>

It seems that there are two factors concerning incorporation of heme into apoglobin; one is binding of heme iron to His F8 and the other is hydrophobic interactions between the heme and the nearby amino acid residues. Heme orientation of Hb A is mostly normal. However, in those of the reconstituted Hb prepared from hemin and apoHb, or rHb expressed in *E. coli*, initially both the normal heme and reversed one are present with a ratio of  $\sim 1:1$ .<sup>11-13,18</sup> It is likely that there exists a mechanism to incorporate the heme into apoHb in the normal orientation *in vivo*. As there is no such system *in vitro* reconstitution or rHb expressed in *E. coli*, both the heme orientations, the normal and reversed ones, could exist.

In the cavity mutant Hbs, heme incorporation into the mutated subunits would be regulated only by hydrophobic interactions, and therefore, no reversed orientation of heme might occur. It is interesting that most native subunits of the cavity mutant Hbs contain normal heme orientation.

We reached two conclusions from the present observations mentioned above.

1. His F8 influences the heme orientation of Hb.
2. Heme orientation of one type of subunits is coupled with the heme orientation of the complementary subunits.

We discuss conclusion (1) as follows:

Recombinant Hb A contains both the normal and reversed hemes in both subunits, while cavity mutant Hbs contain mainly normal orientation of heme in both native and mutated subunits. From these results, we concluded that Fe-His F8 linkage influences the heme orientation. Usually heme orientation must be determined at the moment when the heme binds to His F8 and the possibility to bind normal or reversed heme is equal in the case of apoHb.

We discuss conclusion (2) as follows: We found an interesting phenomenon that the heme orientation of one type of subunits causes the complementary subunits to be almost the same orientation. As shown in the previous article, we could separate rHb A with normal and reversed hemes into Hb with mostly normal orientation (SP-1, normal and reversed with a ratio of 9:1) and that with mostly reversed orientation (SP-3, normal and reversed with a ratio 1:9) by SP Sepharose column chromatography.<sup>18</sup> SP-2 which was eluted between SP-1 and SP-3 contained both the normal and reversed heme with an average ratio of 5:5.<sup>18</sup> However, we point out here that SP-2 is not a mixture of SP-1 and SP-3, but consists of two kinds of dimers, that is, one having only the normal heme and the other having only the reversed heme. These experimental results indicated that heme orientation in one type of subunits influences the heme orientation of the other subunits to be the same with each other within an  $\alpha\beta$  dimer.

Furthermore, our present observation on the heme orientation of the cavity mutant Hbs also seems to give evidence of phenomenon that the heme orientation of one type of subunits causes the complementary subunits to have almost the same orientation. Previously it was suggested that interactions between  $\alpha$  and  $\beta$  subunits affect the orientation of heme by Ishimori and Morishima.<sup>13</sup> They insist that, for instances, no heme pocket of the  $\beta$  subunit in  $\alpha$ -semi Hb ( $\alpha(\text{heme})\beta(\text{no heme})$ ) is different from that of the  $\beta$  subunit in apoHb by quaternary or tertiary structure changes of the  $\beta$  subunit owing to heme insertion (azido-hemin) to the  $\alpha$  subunit. Heme insertion to the  $\beta$  subunit of  $\alpha$ -semi Hb results mostly in the normal heme, while that to apoHb leads to a mixture of both the normal and reversed hemes with ratios of 7:3 and 6:4 in  $\alpha$  subunit and  $\beta$  subunits. Here we would like to address similarity between the heme orientational disorder of the  $\beta$  subunit in  $\alpha$ -semi Hb and that of  $\beta$  subunit in rHb( $\alpha\text{H87G}$ ) in which the  $\alpha$  subunit has already contained the heme,  $\alpha(\text{Im-heme})\beta(\text{no heme})$ .

In rHb( $\beta\text{H92G}$ ), a small amount of the reverse forms was observed, different from the case of rHb( $\alpha\text{H87G}$ ). In this case, again we consider that the structure of  $\alpha$  subunit in  $\beta$ -semi Hb is similar to that of  $\alpha$  subunit in rHb( $\beta\text{H92G}$ ) ( $\alpha(\text{no heme})\beta(\text{heme})$ ) in which the  $\beta$  subunit has already contained the heme. Ishimori and Morishima<sup>13</sup> showed that heme (azido-hemin) insertion to  $\beta$ -semi Hb produces normal and reversed forms with a ratio of 6:4 in the native  $\alpha$  subunit. Thus

reversed form in native  $\alpha$  subunit exists in heme (azido-hemin) insertion to native  $\alpha$  subunit in  $\beta$ -semi Hb. As estimation of reversed form in the native  $\alpha$  subunit of rHb( $\beta$ H92G) is 80%, our result of rHb( $\beta$ H92G) in a ratio of normal and reversed forms is consistent qualitatively with that of  $\beta$ -semi Hb of Ishimori and Morishima.<sup>13</sup>

Our results may indicate the existence of  $\alpha$ (Im-heme) $\beta$ (no heme) and  $\alpha$ (no heme) $\beta$ (Im-heme) as intermediate states, similar to  $\alpha$ -semi Hb and  $\beta$ -semi Hb, based on interpretation by Ishimori and Morishima, respectively.<sup>13</sup> This suggests that heme insertion to heme cavity in the absence of His F8 is faster than that in the presence of His F8.

### Heme-Heme Interaction with and without His F8

Based on the X-ray crystal structure, Perutz proposed a model for cooperativity in which the bond between the His F8 and protein couples heme rearrangements to protein structure rearrangements.<sup>40</sup> To test of the role of proximal His in the Perutz model for cooperativity, the cavity mutant Hbs were first constructed by Barrick *et al.*<sup>21,41</sup> and its ligand binding properties, near-UV CD and <sup>1</sup>H NMR spectra were examined. The cavity mutant Hbs reduces cooperativity and inhibits quaternary structure transition in accord with Perutz model. However, Barrick *et al.* found that some residual allostery may still be operative and suggested that additional heme communication pathways that are not involved with the His F8 pathways through inter- and intra-

dimer interactions within an  $\alpha_2\beta_2$  tetramer exist.<sup>21,41</sup>

Our present finding that heme orientation of one subunit influences that of the other subunit in the cavity mutant Hbs through intradimer interaction within an  $\alpha\beta$  dimer indicates another possible pathway to heme-heme interaction without His F8, and provides a new information on the structure-function relationship of Hb.

### CONCLUSION

Recombinant Hb A adopts two different heme orientations; one is the normal orientation found in native Hb A, and the other one is the reversed orientation in which heme is rotated by 180° about the 5,15-meso axis, relative to the protein moiety. On the other hand, it has been characterized by CD, <sup>1</sup>H NMR and RR spectroscopies that the cavity mutant rHbs in which glycine is substituted for the proximal His (His F8) in either  $\alpha$  or  $\beta$  subunits have mainly the normal heme orientation in both the mutated and native subunits. These results indicate that the heme Fe-His F8 linkage in both  $\alpha$  and  $\beta$  subunits greatly influences the heme orientation and that in addition, the heme orientation of one type of subunits influences the heme orientation of the complementary subunits to be the same. The present study showed that CD and RR spectroscopies also provided powerful tools for the examination of the heme rotational disorder of Hb A, in addition to usual <sup>1</sup>H NMR technique.

### ACKNOWLEDGEMENTS



We thank Professor Chien Ho for the gift of an expression plasmid of Hb, pHE7. The authors are grateful to Ms. Suzuko Araki for the  $^1\text{H}$  NMR measurements of cavity mutant Hbs. We are also grateful to the Medical Center at University of Tsukuba for the gift of concentrated red cell to advance this human Hb study. T.O. is a visiting scientist at RIKEN.

### SUPPORTING INFORMATION

Additional supporting information may be found in the online version of this article at the publisher's web-site.

### LITERATURE CITED

- Jin Y, Sakurai H, Nagai Y, Nagai M. Changes of near-UV CD spectrum of human hemoglobin upon oxygen binding: A study of mutants at  $\alpha 42$ ,  $\alpha 140$ ,  $\beta 145$  tyrosine or  $\beta 37$  tryptophan. *Biopolymers* **2004**; 74:60-63.
- Aki-Jin Y, Nagai Y, Imai K, Nagai M. Changes of near-UV circular dichroism spectra of human hemoglobin upon the R  $\rightarrow$  T quaternary structure transition. In: Kneipp K, Aroca R, Kneipp H, Wentrup-Byrne E, editors. ACS Symposium Series 963: *New Approaches in Biomedical Spectroscopy*. Washington DC: American Chemical Society; **2007**. p 297-311.
- Nagai M, Sugita Y, Yoneyama Y. Circular dichroism of hemoglobin and its subunits in the Soret region. *J Biol Chem* **1969**; 244:1651-1658.
- Sugita Y, Nagai M, Yoneyama Y. Circular dichroism of hemoglobin in relation to the structure surrounding the heme. *J Biol Chem* **1971**; 246:383-388.
- Nagai M, Sugita Y, Yoneyama Y. Oxygen equilibrium and circular dichroism of Hemoglobin-Rainier ( $\alpha_2\beta_2^{145\text{Tyr} \rightarrow \text{Cys}}$ ). *J Biol Chem* **1972**; 247:285-290.
- Li R, Nagai Y, Nagai M. Contribution of  $\alpha 140\text{Tyr}$  and  $\beta 37\text{Trp}$  to the near-UV CD spectra on quaternary structure transition of human hemoglobin A. *Chirality* **2000**; 12:216-220.
- Li R, Nagai Y, Nagai M. Changes of tyrosine and tryptophan residues in human hemoglobin by oxygen binding: Near- and far-UV circular dichroism of isolated chains and recombined hemoglobin. *J Inorg Biochem* **2000**; 82:93-101.
- Nagai M, Nagatomo S, Nagai Y, Ohkubo K, Imai K, Kitagawa T. Near-UV circular dichroism and UV resonance Raman spectra of individual tryptophan residues in human hemoglobin and their changes upon the quaternary structure transition. *Biochemistry* **2012**; 51:5932-5941.
- Nagatomo S, Nagai M, Ogura T, Kitagawa T. Near-UV circular dichroism and UV resonance Raman spectra of tryptophan residues as a structural marker of proteins. *J Phys Chem B* **2013**; 117:9343-9353.
- Nagai M, Nagai Y, Imai K, Neya S. Circular dichroism of hemoglobin and myoglobin. *Chirality* **2014**; 26:78-82.
- La Mar GN, Yamamoto Y, Jue T, Smith KM, Pandey RK.  $^1\text{H}$  NMR characterization of metastable and equilibrium heme orientational

- heterogeneity in reconstituted and native human hemoglobin. *Biochemistry* **1985**; 24:3826-3831.
12. Yamamoto Y, La Mar GN. <sup>1</sup>H NMR study of dynamics and thermodynamics of heme rotational disorder in native and reconstituted hemoglobin A. *Biochemistry* **1986**; 25:5288-5297.
  13. Ishimori K, Morishima I. Study of the specific heme orientation in reconstituted hemoglobins. *Biochemistry* **1988**; 27:4747-4753.
  14. Jue T, La Mar GN. Heme orientational heterogeneity in deuterohemin-reconstituted horse and human hemoglobin characterized by proton nuclear magnetic resonance spectroscopy. *Biochem Biophys Res Commun* **1984**; 119:640-645.
  15. La Mar GN, Jue T, Nagai K, Smith KM, Yamamoto Y, Kauten RJ, Thanabal V, Langry KC, Pandey RK, Leung HK. <sup>1</sup>H-NMR heme resonance assignments by selective deuteration in low-spin complexes of ferric hemoglobin A. *Biochem Biophys Acta* **1988**; 952:131-141.
  16. Shen TJ, Ho NT, Zou M, Sun DP, Cottam PF, Simplaceanu V, Tam MF, Bell DA, Ho C. Production of human normal adult and fetal hemoglobins in *Escherichia coli*. *Protein Eng* **1997**; 10:1085-1097.
  17. Shen TJ, Ho NT, Simplaceanu V, Zou M, Green BN, Tam MF, Ho C. Production of unmodified human adult hemoglobin in *Escherichia coli*. *Proc Natl Acad Sci USA* **1993**; 90:8108-8112.
  18. Nagai M, Nagai Y, Aki Y, Imai K, Wada Y, Nagatomo S, Yamamoto Y. Effect of reversed heme orientation on circular dichroism and cooperative oxygen binding of human adult hemoglobin. *Biochemistry* **2008**; 47:517-525.
  19. Nagatomo S, Nagai Y, Aki Y, Sakurai H, Imai K, Mizusawa N, Ogura T, Kitagawa T, Nagai M. An origin of cooperative oxygen binding of human adult hemoglobin: Different roles of the  $\alpha$  and  $\beta$  subunits in the  $\alpha_2\beta_2$  tetramer. *PLoS ONE* **2015**; 10:e0135080.
  20. Barrick D. Replacement of the proximal ligand of sperm whale myoglobin with free imidazole in the mutant His-93  $\rightarrow$  Gly. *Biochemistry* **1994**; 33:6546-6554.
  21. Barrick D, Ho NT, Simplaceanu V, Dahlquist FW, Ho C. A test of the role of the proximal histidines in the Perutz model for cooperativity in haemoglobin. *Nature Struct Biol* **1997**; 4: 78-83.
  22. Nagai M, Kaminaka S, Ohba Y, Nagai Y, Mizutani Y, Kitagawa T. Ultraviolet resonance Raman studies of quaternary structure of hemoglobin using a tryptophan  $\beta$ 37 mutant. *J Biol Chem* **1995**; 270:1636-1642.
  23. Chen Z, Ruffner DE. Amplification of closed circular DNA *in vitro*. *Nucleic Acid Res* **1998**; 26:1126-1127.
  24. La Mar GN, Davis NL, Parish DW, Smith KM. Heme orientation disorder in reconstituted and native sperm whale myoglobin. Proton nuclear magnetic resonance characterizations by heme methyl deuterium labeling in the met-cyano protein. *J Mol Biol* **1983**; 168:887-896.
  25. Smith KM, Fujinari EM, Langry KC, Parish

- DW, Tabba HD. Manipulation of vinyl groups in protoporphyrin IX: Introduction of deuterium and carbon-13 labels for spectroscopic studies. *J Am Chem Soc* **1983**; 105:6638-6646.
26. Nagai M, Kobayashi C, Nagai Y, Imai K, Mizusawa N, Sakurai H, Neya S, Kayanuma M, Shoji M, Nagatomo S. Involvement of propionate side chains of the heme in circular dichroism of myoglobin: Experimental and theoretical analyses. *J Phys Chem B* **2015**; 119:1275-1287.
27. Park SY, Yokoyama T, Shibayama N, Shiro Y, Tame JRH. 1.25 Å resolution crystal structures of human haemoglobin in the oxy, deoxy, and carbonmonoxy forms. *J Mol Biol* **2006**; 360:690-701.
28. Hu S, Smith KM, Spiro TG. Assignment of protoheme resonance Raman spectrum by heme labeling in myoglobin, *J Am Chem Soc* **1996**; 118:12638-12646.
29. Kitagawa T. The heme protein structure and the iron histidine stretching mode. In: Spiro TG, editor. *Biological Applications of Raman spectroscopy, Vol.3* John Wiley and Sons; **1988**. p 97-131.
30. Kitagawa T, Nagai K, Tsubaki M. Assignment of the Fe-N<sub>ε</sub>(His F8) stretching band in the resonance Raman spectra of deoxymyoglobin. *FEBS Lett* **1979**; 104:376-378.
31. Rwere F, Mak PJ, Kincaid JR. The impact of altered protein-heme interactions on the resonance Raman spectra of heme proteins. Studies of heme rotational disorder. *Biopolymers* **2008**; 89:179-186.
32. Rwere F, Mak PJ, Kincaid JR. Resonance Raman interrogation of the consequences of heme rotational disorder in myoglobin and its ligated derivatives. *Biochemistry* **2008**; 47:12869-12877.
33. Nagai K, Kitagawa T, Morimoto H. Quaternary structures and low frequency molecular vibrations of haems of deoxy and oxyhaemoglobin studied by resonance Raman scattering. *J Mol Biol* **1980**; 136:271-289.
34. Nagai K, Kitagawa T. Differences in Fe(II)-N<sub>ε</sub>(His-F8) stretching frequencies between deoxyhemoglobins in the two alternative quaternary structures. *Proc Natl Acad Sci USA* **1980**; 77:2033-2037.
35. Matsukawa S, Mawatari K, Yoneyama Y, Kitagawa T. Correlation between the iron-histidine stretching frequencies and oxygen affinity of hemoglobins. A continuous strain model. *J Am Chem Soc* **1985**; 107:1108-1113.
36. Teraoka J, Kitagawa T. Structural implication of the heme-linked ionization of horseradish peroxidase probed by the Fe-histidine stretching Raman line. *J Biol Chem* **1981**; 256:3969-3977.
37. Hori H, Kitagawa T. Iron-ligand stretching band in the resonance Raman spectra of ferrous iron porphyrin derivatives. Importance as a probe band for quaternary structure of hemoglobin. *J Am Chem Soc* **1980**; 102:3608-3613.
38. Podstawka E, Rajani C, Kincaid JR, Proniewicz LM. Resonance Raman studies of heme structural differences in subunits of deoxy hemoglobin. *Biopolymers* **2000**;

- 57:201-207.
39. Perutz MF, Muirhead H, Cox JM, Goaman LCG. Three-dimensional Fourier synthesis of horse oxyhaemoglobin at 2.8 Å resolution: the atomic model. *Nature* **1968**; 219:131-139.
40. Perutz MF. Stereochemistry of cooperative effects in haemoglobin: Haem-haem interaction and the problem of allostery. *Nature* **1970**; 228: 726-734.
41. Barrick D, Ho NT, Simplaceanu V, Ho C. Distal ligand reactivity and quaternary structure studies of proximally detached hemoglobins. *Biochemistry* **2001**; 40:3780-3795.
42. Neya S, Morishima I. Interaction of methemoglobin with inositol hexaphosphate. *J Biol Chem* **1981**; 256:793-798.
43. La Mar GN, Burns PD, Jackson JT, Smith KM, Langry KC. Proton magnetic resonance determination of the relative heme orientations in disordered native and reconstituted ferricytochrome *b<sub>5</sub>*. *J Biol Chem* **1981**; 256:6075-6079.

## **Heme Orientation of Cavity Mutant Hemoglobins (His F8→Gly) in Either $\alpha$ or $\beta$ Subunits: Circular Dichroism, $^1\text{H}$ NMR, and Resonance Raman Studies**

MASAKO NAGAI, YUKIFUMI NAGAI, YAYOI AKI, HIROSHI SAKURAI, NAOKI MIZUSAWA,  
TAKASHI OGURA, TEIZO KITAGAWA, YASUHIKO YAMAMOTO, AND SHIGENORI  
NAGATOMO

### **Supporting Information**

#### *Contents*

Figure S1. Absorption spectra of cavity mutant Hbs.

Figure S2. The 413-nm excited RR spectra of Hb A and rHb A with reversed heme in the CO form.

Table S1. Absorption maxima (nm) of cavity mutant Hbs.

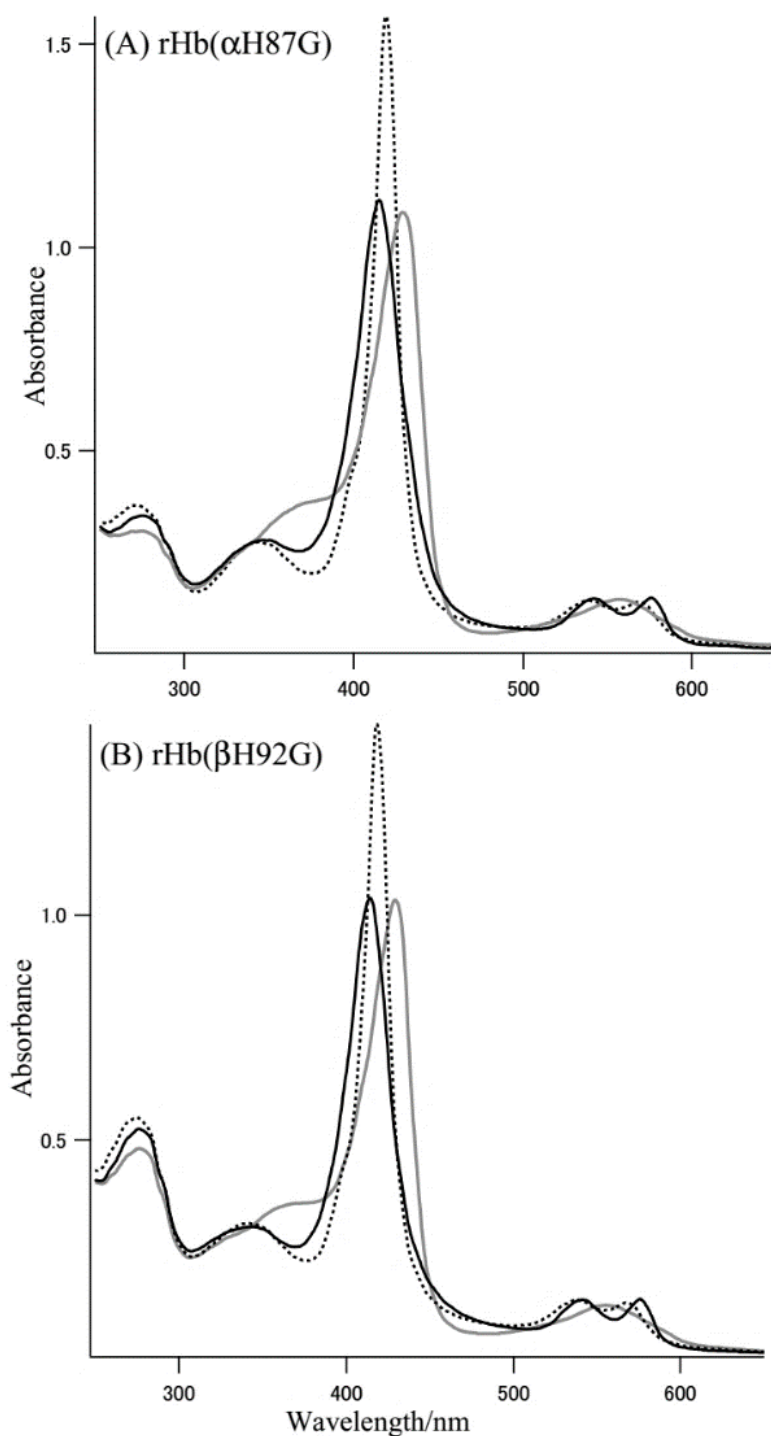


**Fig. S1.** Absorption spectra of cavity mutant Hbs in 0.05 M phosphate buffer (pH 7.0) containing [Im] = 5 mM. (A) rHb( $\alpha$ H87G) and (B) rHb( $\beta$ H92G). Solid black, oxy; solid gray, deoxy; and dotted black, CO forms. Deoxy form of Hb was obtained by adding a small amount of sodium borohydride powder to the Hb solution in Thunberg-type cell after removal of the inside air, oxy form was obtained by introducing air to the deoxy form, and CO-form was obtained by exchanging the inside air to CO gas, respectively.

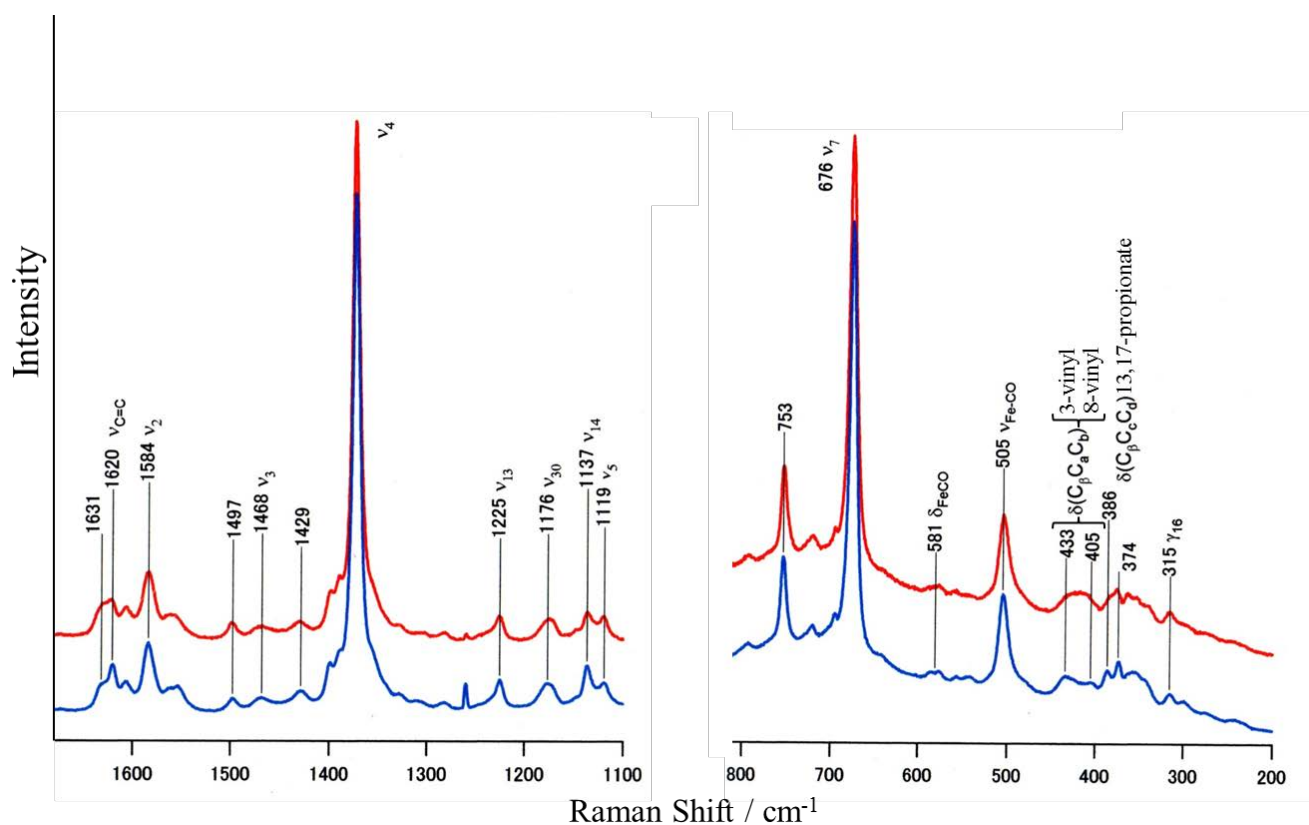


Fig. S2. The 413.1-nm excited RR spectra of Hb A (blue spectrum) and rHb A with the reversed heme (red spectrum) in the CO form. The Hb concentration was 200  $\mu\text{M}$  (in heme) in 0.05 M phosphate buffer, pH 7.0. Left panel, RR spectra in the high frequency region; right panel, RR spectra in the low frequency region. Intensities of RR spectra in the low frequency region are three-fold scaled up relative to those of RR spectra in the high frequency region.

Table S1. Absorption maxima (nm) of cavity mutant hemoglobins in the deoxy-, oxy, and CO-forms in 0.05 M phosphate buffer, pH 7.0 containing 5 mM imidazole.

Hemoglobins	Soret region		Visible region	
Hb A	deoxy	430	555	590 (s)
	oxy	415	542	576.5
	CO	419	538	568
rHb( $\alpha$ H87G)	deoxy	429	557	
	oxy	415	542	576
	CO	419	539	568.5
rHb( $\beta$ H92G)	deoxy	429	554	
	oxy	414	540	575.5
	CO	418	537.5	567.5

s, shoulder



## TOC

